International Endodontic Journal

doi:10.1111/j.1365-2591.2011.01924.x

Uptake of calcium and silicon released from calcium silicate–based endodontic materials into root canal dentine

L. Han & T. Okiji

Division of Cariology, Operative Dentistry and Endodontics, Department of Oral Health Science, Niigata University Graduate School of Medical and Dental Sciences, Niigata, Japan

Abstract

Han L, Okiji T. Uptake of calcium and silicon released from calcium silicate–based endodontic materials into root canal dentine. *International Endodontic Journal*, **44**, 1081–1087, 2011.

Aim To compare Biodentine and White ProRoot mineral trioxide aggregate (MTA) with regard to Ca and Si uptake by adjacent root canal dentine in the presence of phosphate-buffered saline (PBS).

Methodology Root canals of bovine incisor root segments were instrumented, filled with either Biodentine or MTA (n = 20 each) and then immersed in Ca-and Mg-free PBS for 1, 7, 30 or 90 days (n = 5 each). Unfilled, unimmersed dentine specimens (n = 5) served as controls. The specimens were sectioned longitudinally, and the ultrastructure of the dentine–material interface and the elemental composition/distribution in the material–adjacent dentine were analysed using a wavelength-dispersive X-ray spectroscopy electron probe microanalyser with image observation function. Data were statistically analyzed using one-way ANOVA and Tukey's honestly significant difference test or the Mann–Whitney U-test.

Results Along the material–dentine interface, both materials formed a tag-like structure that was composed of either Ca- and P-rich crystalline deposits or the material itself. The width of a Ca- and Si-rich layer detected along the dentine layer of the material–dentine interface showed increases over time. The Ca- and Si-rich layer width was significantly larger ($P < 0.05$) in Biodentine than MTA at 30 and 90 days.

Conclusions Both Biodentine and MTA caused the uptake of Ca and Si in the adjacent root canal dentine in the presence of PBS. The dentine element uptake was more prominent for Biodentine than MTA.

Keywords: bioactivity, Biodentine, calcium, element uptake in dentine, mineral trioxide aggregate, silicon.

Received 6 April 2011; accepted 27 June 2011

Introduction

Mineral trioxide aggregate (MTA) is a calcium silicate–based endodontic material that has been developed by modification of Portland cement (Camilleri *et al.* 2005, Dammaschke *et al.* 2005). A number of laboratory and *in vivo* studies have demonstrated that MTA possesses excellent biocompatibility and sealing ability (Torabinejad & Parirokh 2010); thus, it is currently considered the most promising material for various treatments such as root-end filling (Chong *et al.* 2003, Saunders 2008, Baek *et al.* 2010), direct pulp capping (Nair *et al.* 2008, Okiji & Yoshiba 2009, Mente *et al.* 2010), perforation repair (Main *et al.* 2004) and apical barrier for teeth with necrotic pulps and open apexes (Simon *et al.* 2007).

The bioactivity of MTA has been attributed to its ability to produce surface apatite crystals when in contact with phosphate solutions such as phosphate-buffered saline (PBS) (Sarkar *et al.* 2005, Bozeman *et al.* 2006, Tay *et al.* 2007, Reyes-Carmona *et al.* 2009, Gandolfi *et al.* 2010, Han *et al.* 2010). The crystalline precipitates are formed through interaction of Ca and OH ions released from set MTA (Camilleri 2008a) with phosphates and have been identified as

Correspondence: Linlin Han, Niigata University Graduate School of Medical and Dental Sciences, 5274 Gakkocho-dori, 2-ban-cho, Chuo-ku, Niigata 951-8514, Japan (Tel.:Fax: +81252272865, e-mail: han4378@yahoo.co.jp).

calcium-deficient B-type carbonated apatite precipitates produced via an amorphous calcium phosphate phase (Tay *et al.* 2007). Moreover, apatite crystal formation has also been demonstrated along the MTA–dentine interface and within the interfacial dentine (Sarkar *et al.* 2005, Reyes-Carmona *et al.* 2009, 2010). These findings lead to the notion that apatite formation contributes to leakage reduction not only by filling the gap along the interface but also via dentine interactions such as intrafibrillar apatite deposition. This is supported by the finding that immersion in PBS decreases marginal leakage of MTA apical plugs (Martin *et al.* 2007).

Several new calcium silicate–based materials have recently been developed (Asgary *et al.* 2008, Camilleri 2008b, Gandolfi *et al.* 2008, Gomes-Filho *et al.* 2009), aiming to improve some MTA drawbacks such as its difficult handling property (Johnson 1999) and long setting time (Torabinejad *et al.* 1995, Dammaschke *et al.* 2005). Biodentine (Septodont, Saint Maur des Fossés, France) is amongst these materials and is claimed to be used as a dentine restorative material in addition to endodontic indications similar to those of MTA. Biodentine powder is mainly composed of tricalcium silicate, calcium carbonate and zirconium oxide as the radio-pacifier, whilst Biodentine liquid contains calcium chloride as the setting accelerator and water-reducing agent (Laurent *et al.* 2008). Biodentine shows apatite formation after immersion in phosphate solution (Goldberg *et al.* 2009), indicative of its bioactivity.

Dentine may uptake several elements released from bioactive materials, and such a phenomenon may cause chemical and structural dentine modification resulting in acquisition of higher acid resistance and remineralisation (Hotta *et al.* 2001). The element incorporation by adjacent dentine may also be regarded as an indicator of the material's bioactivity. However, information is limited regarding how the elements released from different calcium silicate–based materials are incorporated in the dentine in contact with these materials. Thus, the aim of this study was to compare Biodentine and MTA with regard to Ca and Si uptake by the adjacent root canal dentine in the presence of PBS.

Material and methods

This study used two commercially available calcium silicate cements: Biodentine™ (Septodont, Saint-Maur-des Fosses, France, Lot: 48032) and White ProRoot MTA (MTA; Dentsply Tulsa Dental, Tulsa, OK, USA, Lot: 08003395).

Sample preparation

Bovine incisors obtained from a Japanese slaughterhouse were used throughout this study. The study exerted no influence on the animal's fate at any stage. Bovine incisor roots were sectioned at the coronal (approximately 4 mm below the cementoenamel junction) and apical (approximately 8 mm above the apex) levels, and the resulting root segments were further ground to 4-mm lengths. The canals of these cylindrical specimens were instrumented using a size 140 K-file (Mani, Tochigi, Japan) under copious irrigation by using 3% sodium hypochlorite (Neo Cleaner; Neo Dental, Tokyo, Japan). The canals were then irrigated with 18% ethylenediaminetetraacetic acid (Ultradent, South Jordan, UT, USA) followed by 3% sodium hypochlorite for 1 min each, washed immediately with purified water and dried using absorbent paper points (VDW, Munich, Germany). These specimens were assigned to one of three groups: Biodentine (n = 20); MTA (n = 20); and unfilled, unimmersed dentine specimens (n = 5).

Biodentine and MTA were mixed according to the manufacturers' instructions and inserted into the prepared root canal specimens by using an appropriate root canal condenser (YDM, Tokyo, Japan). The specimens were stored for 2 h at 100% relative humidity to allow initial setting of the materials and then immersed individually in plastic vials containing 20 mL of Ca- and Mg-free PBS (136.4 mmol L^{-1} NaCl, 2.7 mmol L^{-1} KCl, 8.2 mmol L^{-1} NaH_2PO_4 and 1.25 mmol L^{-1} KH_2PO_4 in 1000 mL of distilled water; pH 7.4) for 1, 7, 30 or 90 days (n = 5, in each period). The immersion solution was replaced every 7 days for the long-term immersion specimens.

After the given periods of time, the specimens were sectioned longitudinally into two symmetrical pieces. One of the two halves was processed for morphological observation, element mapping and chemical analysis along the dentine–material interface, whilst the other half was saved for scanning of the elemental incorporation depth within the root canal dentine as described later.

Morphological and element analysis

The specimens were mounted on aluminium stubs, sputter-coated with a 300-Å-thick gold layer with an ion coater (IC-50; Shimadzu, Kyoto, Japan) and analysed using a wavelength-dispersive X-ray spectroscopy electron probe microanalyser with an image

observation function (SEM-EPMA, EPMA1601; Shimadzu, Kyoto, Japan).

For the morphological observation, the outermost dentine layers of the dentine–material interface were analysed under SEM-EPMA at an accelerating voltage of 15 kV.

Chemical component bulk analysis and element mapping was carried out using SEM-EPMA for the outermost dentine area (60–70 μm away from the interface). The incorporation depths of Ca and Si into the dentine were measured using the elemental line scan from the interface to the direction of inner dentine in the range of 300–500 μm.

Statistical analysis

Data obtained were recorded and analysed using one-way ANOVA and Tukey's honestly significant difference (HSD) test or the Mann–Whitney *U*-test with a significance level of 5%.

Results

Scanning electron microscopy (SEM) analysis revealed the presence of an 'interfacial layer,' which was identified as a 'brighter area' under the back-scattered electron imaging on the longer PBS immersion specimen (Figs 1 and 2) and a tag-like structure within the dentinal tubules along the dentine–material interface (Fig. 1). Part of the brighter area on the interfacial layer and the tag-like structure was subjected to chemical composition analysis and was revealed to be involved in the Ca and Si increases. The interfacial layer appears brighter in the longer period PBS immersion specimens (Figs 1 and 2).

Results of the bulk chemical analyses on the interfacial dentine layer over the 90-day PBS immersion period are shown in Table 1 (Biodentine) and Table 2 (MTA). In control (unfilled) dentine specimens, Ca, O, P and C were detected as the principal elemental dentine components. Following PBS immersion, the relative concentration of these elements showed some changes, most notably increases in Si concentration and Ca/P ratio. In both the Biodentine and MTA specimens, the Ca/P ratio showed significant increases at all the time points compared with those of the control ($P < 0.05$, one-way ANOVA and Tukey's HSD test). Moreover, Si percentages increased in both Biodentine and MTA with time, although Si was not detected in the control dentine specimens.

Element mapping revealed that Ca- and Si-rich dentine areas were observed along the dentine–material interface (Fig. 2). On the other hand, as shown in Table 3, the Biodentine and MTA specimens showed increased incorporation depths as the immersion periods increased. The Ca depth was constantly larger than the Si depth. Moreover, Biodentine specimens constantly showed larger values versus the corresponding MTA specimen values, and significant differences were noted at all time points for Ca and only at 30 and 90 days for Si ($P < 0.05$, Mann–Whitney *U*-test).

Discussion

The present results demonstrated the uptake of Ca and Si in the dentine in contact with both Biodentine and MTA occurred following PBS immersion. This may represent the biomineralisation ability of these calcium silicate materials promoted by the interaction with dentine in the presence of phosphate-containing solutions (Sarkar *et al.* 2005, Reyes-Carmona *et al.* 2009, 2010). Ca and Si uptake most probably causes chemical and structural modification of dentine, which may result in higher acid resistance and physical strength.

The present results also demonstrated that Biodentine may have a more prominent biomineralisation ability than MTA, as Biodentine specimens showed wider Ca- and Si-rich dentine areas (Fig. 2) and larger incorporation depths (Table 3) than MTA revealed by element mapping and line-scan analysis, respectively.

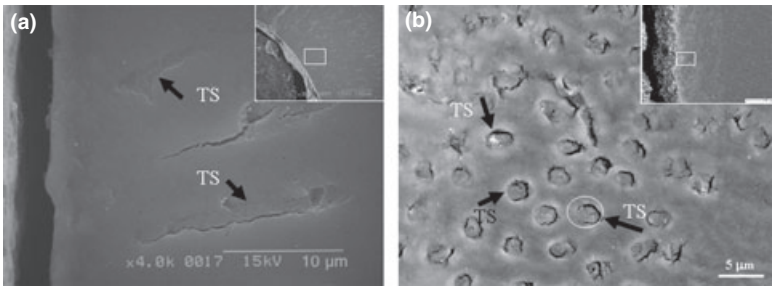

Figure 1 Representative SEM micrographs of the Biodentine–dentine interface after 24 h (a) and 30 days (b) of phosphate-buffered saline immersion. Insets show lower magnification images and boxed areas depict the areas enlarged. TS: tag-like structure. (a) Bar, 10 μm; in inset, 100 μm. (b) Bar, 5 μm; in inset, 50 μm.

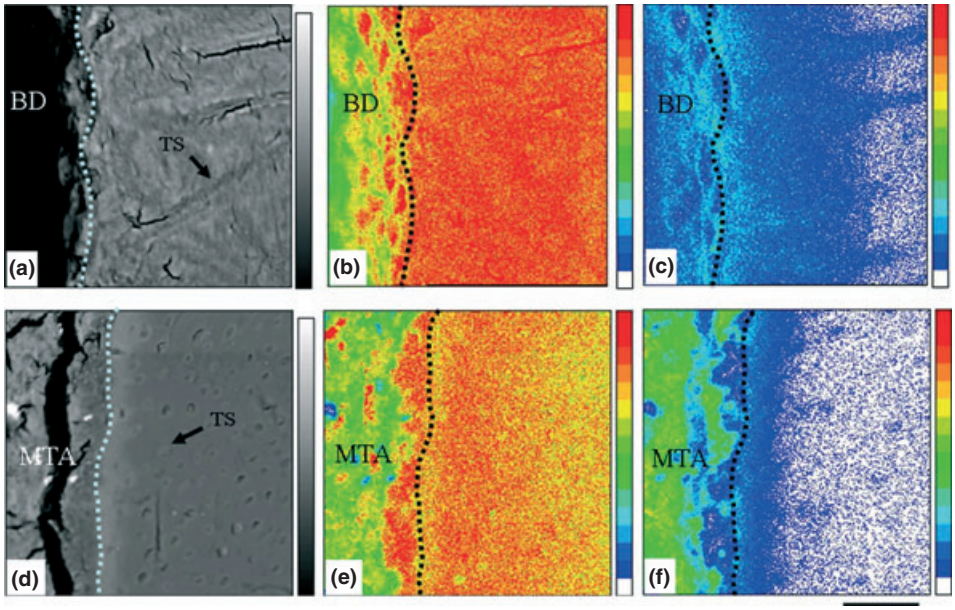

Figure 2 SEM micrographs (a, d) and mapping images for Ca (b, e) and Si (c, f) obtained by SEM-EPMA. Biodentine (BD)–dentine (a, b, c) and mineral trioxide aggregate (MTA)–dentine (d, e, f) interfacial areas of representative specimens after 30-day phosphate-buffered saline immersion. TS: tag-like structure. Dotted lines show the approximate interface position (bar, 20 μm; grey and colour bars, X-ray strength).

Table 1 Principal composition of the interfacial dentine layer of the Biodentine group (atomic %)

		Phosphate-buffered saline immersion			
Elements	Control	24 h	7 days	30 days	90 days
Ca	32.3 (0.3)	42.8 (4.1)	43.9 (3.6)	43.7 (4.3)	44.9 (7.2)
O	26.8 (0.3)	22.9 (4.5)	24.4 (4.6)	23.9 (5.4)	22.1 (2.1)
P	26.5 (1.0)	22.7 (3.1)	21.1 (3.2)	21.7 (3.3)	21.9 (3.3)
C	12.1 (1.0)	9.0 (2.4)	7.4 (1.4)	7.0 (1.8)	6.3 (1.5)
Si	0.0 (0.0)	0.7 (0.2)	1.2 (0.2)	1.7 (0.2)	3.2 (0.2)
Ca/P	1.2 (0.1)a	1.9 (0.1)b	2.1 (0.2)b	2.0 (0.1)b	2.1 (0.2)b

Mean (SD), $n = 5$.
Mean values followed by different letters (Ca/P) are significantly different ($P < 0.05$).

Table 2 Principal composition of the interfacial dentine layer of the mineral trioxide aggregate group (atomic %)

		Phosphate-buffered saline immersion			
Elements	Control	24 h	7 days	30 days	90 days
Ca	32.3 (0.3)	36.3 (6.0)	37.1 (6.2)	37.9 (6.4)	40.2 (5.6)
O	26.8 (0.3)	27.6 (5.9)	28.8 (4.1)	25.2 (1.7)	24.7 (5.0)
P	26.5 (1.0)	23.0 (3.3)	22.6 (3.2)	23.1 (4.4)	23.1 (3.5)
C	12.1 (1.0)	8.9 (0.4)	7.1 (1.0)	9.8 (1.4)	7.5 (1.1)
Si	0.0 (0.0)	1.0 (0.2)	0.8 (0.1)	1.0 (0.7)	1.2 (0.2)
Ca/P	1.2 (0.1)a	1.6 (0.3)ab	1.7 (0.2)b	1.7 (0.2)b	1.8 (0.2)b

Mean (SD), $n = 5$.
Mean values followed by different letters (Ca/P) are significantly different ($P < 0.05$).

This could be because of the amount of Ca and Si dissolution that could be larger in Biodentine than in MTA.

Chemical analysis of the interfacial dentine layer confirmed increased Ca levels and Ca/P ratios in the Biodentine and MTA specimens. This finding is related

Table 3 The incorporation depths of calcium and silicon into the dentine (μm)

Phosphate-buffered saline immersion	Ca		Si	
	Biodentine	MTA	Biodentine	MTA
24 h	66.8 (5.1)a	14.4 (3.8)b	17.6 (2.5)a	13.8 (2.2)a
7 days	116.8 (10.1)a	77.8 (13.5)b	71.2 (10.0)a	61.0 (8.9)a
30 days	212.2 (26.4)a	166.8 (10.1)b	160.2 (16.1)a	115.4 (24.0)b
90 days	296.0 (26.0)a	206.6 (15.1)b	275.8 (28.9)a	171.2 (33.4)b

Mean (SD), $n = 5$.
Mean values followed by different letters in the same line of the same element are significantly different ($P < 0.05$).
MTA, mineral trioxide aggregate.

to Ca incorporation. As such, the quality of the interfacial dentine layer appeared to be improved. On the other hand, Si also accumulated in the same area.

The apatite-forming ability of an artificial material in the presence of phosphate solutions *ex vivo* is regarded as a prerequisite for achieving bonds between the material and living bone (Kokubo & Takadama 2006). It is known that calcium silicate–based ceramic materials commonly exhibit bioactivity to induce bone-like apatite formation (Liu *et al.* 2008); various calcium silicate–based ceramic materials are reported to show such activity, including Portland cement (Tay *et al.* 2007, Reyes-Carmona *et al.* 2009), dicalcium silicate (Gou *et al.* 2005) and tricalcium silicate (Zhao *et al.* 2005). Apatite formation on the calcium silicate–based materials may be attributed to the dissolution of portlandite (calcium hydroxide that formed as a result of hydration reactions of calcium silicate materials); this dissolution causes increased pH and Ca^{2+} ion concentration, which in turn may enhance the supersaturation of phosphate-containing fluid with respect to apatite and, hence, promote precipitation. It has also been described that functional groups, such as Si-OH pre-existing on nanoporous calcium silicate hydrate gel structures formed following hydration reactions, act as nucleation centres for apatite precipitation (Kokubo & Takadama 2006).

Studies on the ultrastructure of the MTA–dentine interface following PBS immersion have demonstrated the formation of a mineral-rich interfacial layer and a tag-like structure extending from the interfacial layer to the dentinal tubules (Sarkar *et al.* 2005, Reyes-Carmona *et al.* 2009). Formation of a 'mineral tag' has also been demonstrated in Biodentine–dentine interfaces (Goldberg *et al.* 2009). The present study confirmed these findings and further demonstrated different tag-like structures with different PBS immersion periods in the relative elemental composition (representative example, Fig. 1). This difference may be attributable to the difference in the amount of Ca release between the PBS immersion periods; Biodentine may release a larger amount of Ca and, consequently, produce larger amounts of calcium phosphate precipitates in the PBS environment. Such a property may have positively influenced the formation of the interfacial layer and the tag-like structure.

Formation of the interfacial layer and tag-like structures may be responsible for the good marginal seal of MTA (Torabinejad & Parirokh 2010). This notion is supported by the finding that immersion in PBS decreases marginal leakage of MTA apical plugs (Martin *et al.* 2007). It has also been reported that immersion of MTA in PBS increases push-out strength (Reyes-Carmona *et al.* 2010), suggesting that the biomineralisation ability confers the material with greater resistance to dislodgement, most likely through the formation of tags, which constitutes micromechanical anchorage. Biodentine is believed to have the potential to exhibit similar characteristics.

This study demonstrated the formation of a Si-rich layer in dentine in contact with Biodentine and MTA. The Si-rich layer was constantly narrower than the Ca-rich layer (Fig. 2), most likely because the amount of Si released from MTA is much smaller than that of Ca (Sarkar *et al.* 2005, Bozeman *et al.* 2006, Camilleri 2008a). The precise role of Si in hard tissue metabolism remains unclear, although it is believed to play a role in the early bone calcification process (Carlisle 1970). Si is also known to enhance the rate of new bone growth when released from bioactive materials *in vivo* (Patel *et al.* 2002). Moreover, Si is reported to induce remineralisation of demineralised dentine *in vitro* (Saito *et al.* 2003). These findings suggest that the release of Si from calcium silicate–based materials may confer additional *in vivo* bioactivity of these materials.

Conclusions

Both Biodentine and MTA caused the uptake of Ca and Si in the adjacent root canal dentine in the presence of

PBS. The elemental uptake into dentine was more prominent for Biodentine than for MTA.

References

Asgary S, Shahabi S, Jafarzadeh T, Amini S, Kheirieh S (2008) The properties of a new endodontic material. *Journal of Endodontics* **34**, 990–3.

Baek SH, Lee WC, Setzer FC, Kim S (2010) Periapical bone regeneration after endodontic microsurgery with three different root-end filling materials: amalgam, SuperEBA, and mineral trioxide aggregate. *Journal of Endodontics* **36**, 1323–5.

Bozeman TB, Lemon RR, Eleazer PD (2006) Elemental analysis of crystal precipitate from gray and white MTA. *Journal of Endodontics* **32**, 425–8.

Camilleri J (2008a) Characterization of hydration products of mineral trioxide aggregate. *International Endodontic Journal* **41**, 408–17.

Camilleri J (2008b) Modification of mineral trioxide aggregate. Physical and mechanical properties. *International Endodontic Journal* **41**, 843–9.

Camilleri J, Montesin FE, Brady K, Sweeney R, Curtis RV, Pitt Ford TR (2005) The constitution of mineral trioxide aggregate. *Dental Materials* **21**, 297–303.

Carlisle EM (1970) Silicon: a possible factor in bone calcification. *Science* **167**, 279–80.

Chong BS, Pitt Ford TR, Hudson MB (2003) A prospective clinical study of mineral trioxide aggregate and IRM when used as root-end filling materials in endodontic surgery. *International Endodontic Journal* **36**, 520–6.

Dammaschke T, Gerth HUV, Züchner H, Schäfer E (2005) Chemical and physical surface and bulk material characterization of white ProRoot MTA and two Portland cements. *Dental Materials* **21**, 731–8.

Gandolfi MG, Pagani S, Perut F *et al.* (2008) Innovative silicate-based cements for endodontics: a study of osteoblast-like cell response. *Journal of Biomedical Materials Research A* **87**, 477–86.

Gandolfi MG, Taddei P, Tinti A, Prati C (2010) Apatite-forming ability (bioactivity) of ProRoot MTA. *International Endodontic Journal* **43**, 917–29.

Goldberg M, Pradelle-Plasse N, Tran X *et al.* (2009) Emerging trends in (bio)material researches. In: Goldberg M, ed. *Biocompatibility or cytotoxic effects of dental composites*. Oxford, UK: Coxmoor Publishing, pp. 181–203.

Gomes-Filho JE, Rodrigues G, Watanabe S *et al.* (2009) Evaluation of the tissue reaction to fast endodontic cement (CER) and Angelus MTA. *Journal of Endodontics* **35**, 1377–80.

Gou Z, Chang J, Zhai W, Wang J (2005) Study on the self-setting property and the in vitro bioactivity of beta-Ca_2SiO_4. *Journal of Biomedical Materials Research B Applied Biomaterials* **73**, 244–51.

Han L, Okiji T, Okawa S (2010) Morphological and chemical analysis of different precipitates on mineral trioxide aggregate immersed in different fluids. *Dental Materials Journal* **29**, 512–7.

Hotta M, Li Y, Sekine I (2001) Mineralization in bovine dentin adjacent to glass-ionomer restorations. *Journal of Dentistry* **29**, 211–5.

Johnson BR (1999) Considerations in the selection of a root-end filling material. *Oral Surgery Oral Medicine Oral Pathology Oral Radiology & Endodontology* **87**, 398–404.

Kokubo T, Takadama H (2006) How useful is SBF in predicting in vivo bone bioactivity? *Biomaterials* **27**, 2907–15.

Laurent P, Camps J, iDe Méo M, Déjou J, About I (2008) Induction of specific cell responses to a Ca_3SiO_5-based posterior restorative material. *Dental Materials* **24**, 1486–94.

Liu X, Morra M, Carpi A, Li B (2008) Bioactive calcium silicate ceramics and coatings. *Biomedicine & Pharmacotherapy* **62**, 526–9.

Main C, Mirzayan N, Shabahang S, Torabinejad M (2004) Repair of root perforations using mineral trioxide aggregate: a long-term study. *Journal of Endodontics* **30**, 80–3.

Martin RL, Monticelli F, Brackett WW *et al.* (2007) Sealing properties of mineral trioxide aggregate orthograde apical plugs and root fillings in an *in vitro* apexification model. *Journal of Endodontics* **33**, 272–5.

Mente J, Geletneky B, Ohle M *et al.* (2010) Mineral trioxide aggregate or calcium hydroxide direct pulp capping: an analysis of the clinical treatment outcome. *Journal of Endodontics* **36**, 806–13.

Nair PNR, Duncan HF, Pitt Ford TR, Luder HU (2008) Histological, ultrastructural and quantitative investigations on the response of healthy human pulps to experimental capping with mineral trioxide aggregate: a randomized controlled trial. *International Endodontic Journal* **41**, 128–50.

Okiji T, Yoshiba K (2009) Reparative dentinogenesis induced by mineral trioxide aggregate: a review from the biological and physicochemical points of view. *International Journal of Dentistry*, doi:10.1155/2009/464280.

Patel N, Best SM, Bonfield M *et al.* (2002) A comparative study on the *in vivo* behavior of hydroxyapatite and silicon substituted hydroxyapatite granules. *Journal of Materials Science: Materials in Medicine* **13**, 1199–206.

Reyes-Carmona JF, Felippe MS, Felippe WT (2009) Biomineralization ability and interaction of mineral trioxide aggregate and white Portland cement with dentin in a phosphate-containing fluid. *Journal of Endodontics* **35**, 731–6.

Reyes-Carmona JF, Felippe MS, Felippe WT (2010) The biomineralization ability of mineral trioxide aggregate and Portland cement on dentin enhances the push-out strength. *Journal of Endodontics* **36**, 286–91.

Saito T, Toyooka H, Ito S, Crenshaw MA (2003) *In vitro* study of remineralization of dentin: effects of ions on mineral induction by decalcified dentin matrix. *Caries Research* **37**, 445–9.

Sarkar NK, Caicedo R, Ritwik P, Moiseyeva R, Kawashima I (2005) Physicochemical basis of the biologic properties of

mineral trioxide aggregate. *Journal of Endodontics* **31**, 97–100.

Saunders WP (2008) A prospective clinical study of periradicular surgery using mineral trioxide aggregate as a root-end filling. *Journal of Endodontics* **34**, 660–5.

Simon S, Rilliard F, Berdal A, Machtou P (2007) The use of mineral trioxide aggregate in one-visit apexification treatment: a prospective study. *International Endodontic Journal* **40**, 186–97.

Tay FR, Pashley DH, Rueggeberg FA, Loushine RJ, Weller RN (2007) Calcium phosphate phase transformation produced by the interaction of the Portland cement component of white mineral trioxide aggregate with a phosphate-containing fluid. *Journal of Endodontics* **33**, 1347–51.

Torabinejad M, Parirokh M (2010) Mineral trioxide aggregate: a comprehensive literature review Part II: leakage and biocompatibility investigations. *Journal of Endodontics* **36**, 190–202.

Torabinejad M, Hong CU, McDonald F, Pitt Ford TR (1995) Physical and chemical properties of a new root-end filling material. *Journal of Endodontics* **21**, 349–53.

Zhao W, Wang J, Zhai W, Wang Z, Chang J (2005) The self-setting properties and *in vitro* bioactivity of tricalcium silicate. *Biomaterials* **26**, 6113–21.